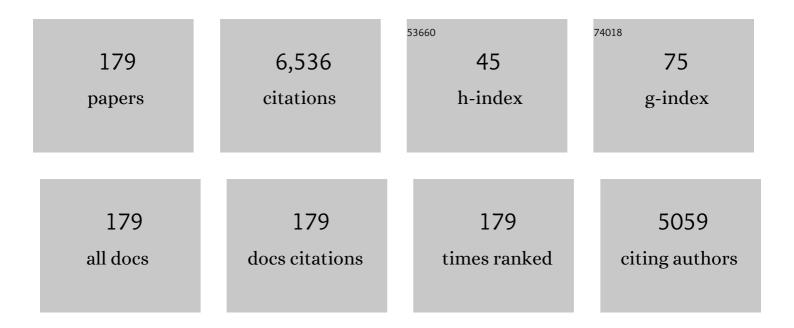
List of Publications by Year in descending order

Source: https://exaly.com/author-pdf/541641/publications.pdf Version: 2024-02-01



7HIMEL HUANC

#	Article	IF	CITATIONS
1	Near-infrared Raman spectroscopy for optical diagnosis of lung cancer. International Journal of Cancer, 2003, 107, 1047-1052.	2.3	724
2	Rapid near-infrared Raman spectroscopy system for real-time in vivo skin measurements. Optics Letters, 2001, 26, 1782.	1.7	243
3	Diagnostic potential of near-infrared Raman spectroscopy in the stomach: differentiating dysplasia from normal tissue. British Journal of Cancer, 2008, 98, 457-465.	2.9	204
4	Raman spectroscopy of in vivo cutaneous melanin. Journal of Biomedical Optics, 2004, 9, 1198.	1.4	197
5	Raman spectroscopy for optical diagnosis in normal and cancerous tissue of the nasopharynx?preliminary findings. Lasers in Surgery and Medicine, 2003, 32, 210-214.	1.1	166
6	<i>In Vivo</i> Diagnosis of Esophageal Cancer Using Image-Guided Raman Endoscopy and Biomolecular Modeling. Technology in Cancer Research and Treatment, 2011, 10, 103-112.	0.8	129
7	High Wavenumber Raman Spectroscopy for in Vivo Detection of Cervical Dysplasia. Analytical Chemistry, 2009, 81, 8908-8915.	3.2	126
8	Simultaneous Fingerprint and High-Wavenumber Confocal Raman Spectroscopy Enhances Early Detection of Cervical Precancer In Vivo. Analytical Chemistry, 2012, 84, 5913-5919.	3.2	123
9	Integrated Raman spectroscopy and trimodal wide-field imaging techniques for real-time in vivo tissue Raman measurements at endoscopy. Optics Letters, 2009, 34, 758.	1.7	120
10	Fiberoptic Confocal Raman Spectroscopy for Real-Time In Vivo Diagnosis of Dysplasia in Barrett's Esophagus. Gastroenterology, 2014, 146, 27-32.	0.6	119
11	Real-time Raman spectroscopy for in vivo, online gastric cancer diagnosis during clinical endoscopic examination. Journal of Biomedical Optics, 2012, 17, 1.	1.4	115
12	Raman Spectroscopy in Combination with Background Near-infrared Autofluorescence Enhances the In Vivo Assessment of Malignant Tissues. Photochemistry and Photobiology, 2005, 81, 1219.	1.3	111
13	Cutaneous melanin exhibiting fluorescence emission under near-infrared light excitation. Journal of Biomedical Optics, 2006, 11, 034010.	1.4	101
14	<i>In vivo</i> diagnosis of gastric cancer using Raman endoscopy and ant colony optimization techniques. International Journal of Cancer, 2011, 128, 2673-2680.	2.3	97
15	Characterizing variability in in vivo Raman spectra of different anatomical locations in the upper gastrointestinal tract toward cancer detection. Journal of Biomedical Optics, 2011, 16, 037003.	1.4	94
16	Raman spectroscopy for optical diagnosis in the larynx: Preliminary findings. Lasers in Surgery and Medicine, 2005, 37, 192-200.	1.1	93
17	In vivo detection of epithelial neoplasia in the stomach using image-guided Raman endoscopy. Biosensors and Bioelectronics, 2010, 26, 383-389.	5.3	90
18	Combining near-infrared-excited autofluorescence and Raman spectroscopy improves in vivo diagnosis of gastric cancer. Biosensors and Bioelectronics, 2011, 26, 4104-4110.	5.3	89

#	Article	IF	CITATIONS
19	Fiberâ€optic Raman spectroscopy probes gastric carcinogenesis <i>in vivo</i> at endoscopy. Journal of Biophotonics, 2013, 6, 49-59.	1.1	87
20	Large eddy simulation of flame structure and combustion mode in a hydrogen fueled supersonic combustor. International Journal of Hydrogen Energy, 2015, 40, 9815-9824.	3.8	87
21	Coherent anti-Stokes Raman scattering microscopy using tightly focused radially polarized light. Optics Letters, 2009, 34, 1870.	1.7	86
22	Raman endoscopy for in vivo differentiation between benign and malignant ulcers in the stomach. Analyst, The, 2010, 135, 3162.	1.7	86
23	Second-Harmonic Generation from Sub-5 nm Gaps by Directed Self-Assembly of Nanoparticles onto Template-Stripped Gold Substrates. Nano Letters, 2015, 15, 5976-5981.	4.5	86
24	In vivo diagnosis of cervical precancer using Raman spectroscopy and genetic algorithm techniques. Analyst, The, 2011, 136, 4328.	1.7	85
25	Diagnosis of gastric cancer using near-infrared Raman spectroscopy and classification and regression tree techniques. Journal of Biomedical Optics, 2008, 13, 034013.	1.4	83
26	Simultaneous fingerprint and highâ€wavenumber fiberâ€optic Raman spectroscopy enhances realâ€time <i>in vivo</i> diagnosis of adenomatous polyps during colonoscopy. Journal of Biophotonics, 2016, 9, 333-342.	1.1	79
27	Detailed numerical simulation of transient mixing and combustion of premixed methane/air mixtures in a pre-chamber/main-chamber system relevant to internal combustion engines. Combustion and Flame, 2018, 188, 357-366.	2.8	79
28	Higher-order coherent anti-Stokes Raman scattering microscopy realizes label-free super-resolution vibrational imaging. Nature Photonics, 2020, 14, 115-122.	15.6	79
29	In vivo early diagnosis of gastric dysplasia using narrow-band image-guided Raman endoscopy. Journal of Biomedical Optics, 2010, 15, 037017.	1.4	77
30	Early detection of biomolecular changes in disrupted porcine cartilage using polarized Raman spectroscopy. Journal of Biomedical Optics, 2011, 16, 017003.	1.4	73
31	Spectroscopic diagnosis of laryngeal carcinoma using near-infrared Raman spectroscopy and random recursive partitioning ensemble techniques. Analyst, The, 2009, 134, 1232.	1.7	66
32	Optical diagnosis of laryngeal cancer using high wavenumber Raman spectroscopy. Biosensors and Bioelectronics, 2012, 35, 213-217.	5.3	66
33	Development of a beveled fiber-optic confocal Raman probe for enhancing in vivo epithelial tissue Raman measurements at endoscopy. Optics Letters, 2013, 38, 2321.	1.7	65
34	Eulerian-Lagrangian modelling of detonative combustion in two-phase gas-droplet mixtures with OpenFOAM: Validations and verifications. Fuel, 2021, 286, 119402.	3.4	65
35	Simulations of combustion oscillation and flame dynamics in a strut-based supersonic combustor. International Journal of Hydrogen Energy, 2017, 42, 8278-8287.	3.8	63
36	Characterizing Variability of In Vivo Raman Spectroscopic Properties of Different Anatomical Sites of Normal Colorectal Tissue towards Cancer Diagnosis at Colonoscopy. Analytical Chemistry, 2015, 87, 960-966.	3.2	62

#	Article	IF	CITATIONS
37	Fiber-optic Raman probe couples ball lens for depth-selected Raman measurements of epithelial tissue. Biomedical Optics Express, 2010, 1, 17.	1.5	56
38	Assessment of liver steatosis and fibrosis in rats using integrated coherent anti-Stokes Raman scattering and multiphoton imaging technique. Journal of Biomedical Optics, 2011, 16, 1.	1.4	56
39	Characterizing variability in <i>in vivo</i> Raman spectroscopic properties of different anatomical sites of normal tissue in the oral cavity. Journal of Raman Spectroscopy, 2012, 43, 255-262.	1.2	56
40	Two-photon graphene quantum dot modified Gd ₂ O ₃ nanocomposites as a dual-mode MRI contrast agent and cell labelling agent. Nanoscale, 2018, 10, 5642-5649.	2.8	56
41	Nearâ€infrared Raman spectroscopy for gastric precancer diagnosis. Journal of Raman Spectroscopy, 2009, 40, 908-914.	1.2	55
42	Saturated Stimulated-Raman-Scattering Microscopy for Far-Field Superresolution Vibrational Imaging. Physical Review Applied, 2019, 11, .	1.5	54
43	Low-level detection of anti-cancer drug in blood plasma using microwave-treated gold-polystyrene beads as surface-enhanced Raman scattering substrates. Biosensors and Bioelectronics, 2010, 26, 580-584.	5.3	53
44	Near-infrared-excited confocal Raman spectroscopy advances <i>in vivo</i> diagnosis of cervical precancer. Journal of Biomedical Optics, 2013, 18, 067007.	1.4	47
45	Classification of colonic tissues using near-infrared Raman spectroscopy and support vector machines. International Journal of Oncology, 0, , .	1.4	46
46	Simultaneous fingerprint and high-wavenumber fiber-optic Raman spectroscopy improves in vivo diagnosis of esophageal squamous cell carcinoma at endoscopy. Scientific Reports, 2015, 5, 12957.	1.6	46
47	Real-time In vivo Diagnosis of Nasopharyngeal Carcinoma Using Rapid Fiber-Optic Raman Spectroscopy. Theranostics, 2017, 7, 3517-3526.	4.6	46
48	Nearâ€infrared Raman spectroscopy for optical diagnosis in the stomach: Identification of <i>Helicobacterâ€pylori</i> infection and intestinal metaplasia. International Journal of Cancer, 2010, 126, 1920-1927.	2.3	45
49	Rapid Fiber-optic Raman Spectroscopy for Real-Time <i>In Vivo</i> Detection of Gastric Intestinal Metaplasia during Clinical Gastroscopy. Cancer Prevention Research, 2016, 9, 476-483.	0.7	45
50	Interferometric polarization coherent anti-Stokes Raman scattering (IP-CARS) microscopy. Optics Letters, 2008, 33, 602.	1.7	44
51	Large eddy simulation of turbulent supersonic hydrogen flames with OpenFOAM. Fuel, 2020, 282, 118812.	3.4	44
52	Combustion oscillation study in a kerosene fueled rocket-based combined-cycle engine combustor. Acta Astronautica, 2016, 129, 260-270.	1.7	41
53	Comparative study of the endoscope-based bevelled and volume fiber-optic Raman probes for optical diagnosis of gastric dysplasia in vivo at endoscopy. Analytical and Bioanalytical Chemistry, 2015, 407, 8303-8310.	1.9	40
54	Flame stabilization mechanism study in a hydrogen-fueled model supersonic combustor under different air inflow conditions. International Journal of Hydrogen Energy, 2017, 42, 21360-21370.	3.8	40

#	Article	IF	CITATIONS
55	Large eddy simulation of combustion characteristics in a kerosene fueled rocket-based combined-cycle engine combustor. Acta Astronautica, 2016, 127, 326-334.	1.7	39
56	Epi-Detected Hyperspectral Stimulated Raman Scattering Microscopy for Label-Free Molecular Subtyping of Glioblastomas. Analytical Chemistry, 2018, 90, 10249-10255.	3.2	36
57	Real-Time Monitoring of Pharmacokinetics of Antibiotics in Biofilms with Raman-Tagged Hyperspectral Stimulated Raman Scattering Microscopy. Theranostics, 2019, 9, 1348-1357.	4.6	36
58	Effect of formalin fixation on the near-infrared Raman spectroscopy of normal and cancerous human bronchial tissues. International Journal of Oncology, 2003, 23, 649.	1.4	33
59	Real-time in vivo diagnosis of laryngeal carcinoma with rapid fiber-optic Raman spectroscopy. Biomedical Optics Express, 2016, 7, 3705.	1.5	33
60	Fiber-optic Raman spectroscopy for in vivo diagnosis of gastric dysplasia. Faraday Discussions, 2016, 187, 377-392.	1.6	33
61	In vivo diagnosis of colonic precancer and cancer using near-infrared autofluorescence spectroscopy and biochemical modeling. Journal of Biomedical Optics, 2011, 16, 067005.	1.4	32
62	<i>In vivo</i> , real-time, transnasal, image-guided Raman endoscopy: defining spectral properties in the nasopharynx and larynx. Journal of Biomedical Optics, 2012, 17, 0770021.	1.4	32
63	Advances in realâ€time fiberâ€optic Raman spectroscopy for early cancer diagnosis: Pushing the frontier into clinical endoscopic applications. Translational Biophotonics, 2021, 3, e202000018.	1.4	32
64	Aqueous phase synthesis of widely tunable photoluminescence emission CdTe/CdS core/shell quantum dots under a totally ambient atmosphere. Journal of Materials Chemistry, 2012, 22, 16336.	6.7	31
65	Fiber-Optic Raman Spectroscopy with Nature-Inspired Genetic Algorithms Enhances Real-Time in Vivo Detection and Diagnosis of Nasopharyngeal Carcinoma. Analytical Chemistry, 2019, 91, 8101-8108.	3.2	31
66	Polarized near-infrared autofluorescence imaging combined with near-infrared diffuse reflectance imaging for improving colonic cancer detection. Optics Express, 2010, 18, 24293.	1.7	30
67	Heterodyne polarization coherent anti-Stokes Raman scattering microscopy. Applied Physics Letters, 2008, 92, 123901.	1.5	28
68	Polarization-resolved hyperspectral stimulated Raman scattering microscopy for label-free biomolecular imaging of the tooth. Applied Physics Letters, 2016, 108, .	1.5	27
69	Modelling n-heptane dilute spray flames in a model supersonic combustor fueled by hydrogen. Fuel, 2020, 264, 116809.	3.4	27
70	SURFACE-ENHANCED RAMAN SCATTERING: PRINCIPLES, NANOSTRUCTURES, FABRICATIONS, AND BIOMEDICAL APPLICATIONS. Journal of Innovative Optical Health Sciences, 2008, 01, 267-284.	0.5	25
71	Circularly polarized coherent anti-Stokes Raman scattering microscopy. Optics Letters, 2013, 38, 1262.	1.7	25
72	Integrated Mueller-matrix near-infrared imaging and point-wise spectroscopy improves colonic cancer detection. Biomedical Optics Express, 2016, 7, 1116.	1.5	25

#	Article	IF	CITATIONS
73	Development of a hybrid Raman spectroscopy and optical coherence tomography technique for real-time in vivo tissue measurements. Optics Letters, 2016, 41, 3045.	1.7	25
74	Real-Time Monitoring of Pharmacokinetics of Mitochondria-Targeting Molecules in Live Cells with Bioorthogonal Hyperspectral Stimulated Raman Scattering Microscopy. Analytical Chemistry, 2020, 92, 740-748.	3.2	25
75	Development of a multiplexing fingerprint and high wavenumber Raman spectroscopy technique for real-time <i>in vivo</i> tissue Raman measurements at endoscopy. Journal of Biomedical Optics, 2013, 18, 030502.	1.4	24
76	Optical diagnosis and characterization of dental caries with polarization-resolved hyperspectral stimulated Raman scattering microscopy. Biomedical Optics Express, 2016, 7, 1284.	1.5	24
77	Numerical investigations of mixed supersonic and subsonic combustion modes in a model combustor. International Journal of Hydrogen Energy, 2020, 45, 1045-1060.	3.8	24
78	Application of the sparse-Lagrangian multiple mapping conditioning approach to a model supersonic combustor. Physics of Fluids, 2020, 32, .	1.6	23
79	Stimulated Raman Scattering Tomography Enables Labelâ€Free Volumetric Deep Tissue Imaging. Laser and Photonics Reviews, 2021, 15, 2100069.	4.4	23
80	Monte Carlo simulation of cutaneous reflectance and fluorescence measurements – The effect of melanin contents and localization. Journal of Photochemistry and Photobiology B: Biology, 2007, 86, 219-226.	1.7	22
81	Beveled fiber-optic probe couples a ball lens for improving depth-resolved fluorescence measurements of layered tissue: Monte Carlo simulations. Physics in Medicine and Biology, 2008, 53, 937-951.	1.6	22
82	Investigations of autoignition and propagation of supersonic ethylene flames stabilized by a cavity. Applied Energy, 2020, 265, 114795.	5.1	22
83	Near-infrared Raman spectroscopy for assessing biochemical changes of cervical tissue associated with precarcinogenic transformation. Analyst, The, 2014, 139, 5379-5386.	1.7	21
84	Real time near-infrared Raman spectroscopy for the diagnosis of nasopharyngeal cancer. Oncotarget, 2017, 8, 49443-49450.	0.8	21
85	On the interactions between a propagating shock wave and evaporating water droplets. Physics of Fluids, 2020, 32, .	1.6	21
86	Laser-induced autofluorescence microscopy of normal and tumor human colonic tissue. International Journal of Oncology, 2004, 24, 59.	1.4	20
87	Lock-in-detection-free line-scan stimulated Raman scattering microscopy for near video-rate Raman imaging. Optics Letters, 2016, 41, 3960.	1.7	20
88	Deep Learning-Guided Fiberoptic Raman Spectroscopy Enables Real-Time <i>In Vivo</i> Diagnosis and Assessment of Nasopharyngeal Carcinoma and Post-treatment Efficacy during Endoscopy. Analytical Chemistry, 2021, 93, 10898-10906.	3.2	20
89	Elliptically polarized coherent anti-Stokes Raman scattering microscopy. Optics Letters, 2008, 33, 2842.	1.7	19
90	Integrated coherent anti-Stokes Raman scattering and multiphoton microscopy for biomolecular imaging using spectral filtering of a femtosecond laser. Applied Physics Letters, 2010, 96, 133701.	1.5	19

#	Article	IF	CITATIONS
91	Near-field effects on coherent anti-Stokes Raman scattering microscopy imaging. Optics Express, 2007, 15, 4118.	1.7	18
92	Radially polarized tip-enhanced near-field coherent anti-Stokes Raman scattering microscopy for vibrational nano-imaging. Applied Physics Letters, 2013, 103, .	1.5	18
93	Improving surface-enhanced Raman scattering effect using gold-coated hierarchical polystyrene bead substrates modified with postgrowth microwave treatment. Journal of Biomedical Optics, 2008, 13, 064040.	1.4	17
94	Near-infrared autofluorescence spectroscopy for in vivo identification of hyperplastic and adenomatous polyps in the colon. Biosensors and Bioelectronics, 2011, 30, 118-122.	5.3	17
95	Spatial light-modulated stimulated Raman scattering (SLM-SRS) microscopy for rapid multiplexed vibrational imaging. Theranostics, 2020, 10, 312-322.	4.6	16
96	Scalable Fourier transform system for instantly structured illumination in lithography. Optics Letters, 2017, 42, 1978.	1.7	16
97	Improved contrast radially polarized coherent anti-Stokes Raman scattering microscopy using annular aperture detection. Applied Physics Letters, 2009, 95, .	1.5	15
98	Numerical study of effects of light polarization, scatterer sizes and orientations on near-field coherent anti-Stokes Raman scattering microscopy. Optics Express, 2009, 17, 2423.	1.7	14
99	Non-invasive analysis of hormonal variations and effect of postmenopausal Vagifem treatment on women using inÂvivo high wavenumber confocal Raman spectroscopy. Analyst, The, 2013, 138, 4120.	1.7	14
100	Multivariate Reference Technique for Quantitative Analysis of Fiber-Optic Tissue Raman Spectroscopy. Analytical Chemistry, 2013, 85, 11297-11303.	3.2	14
101	Polarization-resolved second-harmonic generation imaging for liver fibrosis assessment without labeling. Applied Physics Letters, 2013, 103, .	1.5	14
102	Label-Free Follow-Up Surveying of Post-Treatment Efficacy and Recurrence in Nasopharyngeal Carcinoma Patients with Fiberoptic Raman Endoscopy. Analytical Chemistry, 2021, 93, 2053-2061.	3.2	14
103	Multimodal nonlinear optical microscopic imaging provides new insights into acetowhitening mechanisms in live mammalian cells without labeling. Biomedical Optics Express, 2014, 5, 3116.	1.5	12
104	Characterizing biochemical and morphological variations of clinically relevant anatomical locations of oral tissue in vivo with hybrid Raman spectroscopy and optical coherence tomography technique. Journal of Biophotonics, 2018, 11, e201700113.	1.1	12
105	Diagnosis of early stage nasopharyngeal carcinoma using ultraviolet autofluorescence excitation–emission matrix spectroscopy and parallel factor analysis. Analyst, The, 2011, 136, 3896.	1.7	11
106	Label-free three-dimensional imaging of cell nucleus using third-harmonic generation microscopy. Applied Physics Letters, 2014, 105, 103705.	1.5	11
107	Spectroscopic assessment of dermal melanin using blue vitiligo as an in vivo model. Photodermatology Photoimmunology and Photomedicine, 2006, 22, 46-51.	0.7	10
108	Epi-detected quadruple-modal nonlinear optical microscopy for label-free imaging of the tooth. Applied Physics Letters, 2015, 106, .	1.5	10

ZHIWEI HUANG

#	Article	IF	CITATIONS
109	Ignition and deflagration-to-detonation transition modes in ethylene/air mixtures behind a reflected shock. Physics of Fluids, 2022, 34, .	1.6	10
110	Integrated autofluorescence endoscopic imaging and point-wise spectroscopy for real-time in vivo tissue measurements. Journal of Biomedical Optics, 2010, 15, 1.	1.4	9
111	Effects of scatterers' sizes on near-field coherent anti-Stokes Raman scattering under tightly focused radially and linearly polarized light excitation. Optics Express, 2010, 18, 10888.	1.7	9
112	Half-ball lens couples a beveled fiber probe for depth-resolved spectroscopy: Monte Carlo simulations. Applied Optics, 2008, 47, 3152.	2.1	8
113	Triple-frequency symmetric subtraction scheme for nonresonant background suppression in coherent anti-Stokes Raman scattering (CARS) microscopy. Optics Express, 2010, 18, 15714.	1.7	8
114	Development and characterization of a disposable submillimeter fiber optic Raman needle probe for enhancing real-time in vivo deep tissue and biofluids Raman measurements. Optics Letters, 2021, 46, 5197.	1.7	8
115	Mapping the Intratumoral Heterogeneity in Glioblastomas with Hyperspectral Stimulated Raman Scattering Microscopy. Analytical Chemistry, 2021, 93, 2377-2384.	3.2	8
116	Supercritical focusing coherent anti-Stokes Raman scattering microscopy for high-resolution vibrational imaging. Optics Letters, 2018, 43, 5615.	1.7	8
117	Optimization of extinction efficiency of goldâ€coated polystyrene bead substrates improves surfaceâ€enhanced Raman scattering effects by postâ€growth microwave heating treatment. Journal of Raman Spectroscopy, 2010, 41, 374-380.	1.2	7
118	Annular aperture-detected coherent anti-Stokes Raman scattering microscopy for high contrast vibrational imaging. Applied Physics Letters, 2010, 97, 083701.	1.5	7
119	Real-time depth-resolved fiber optic Raman endoscopy forin vivodiagnosis of gastric precancer. , 2014, , , .		7
120	Quantitative assessment of spinal cord injury using circularly polarized coherent anti-Stokes Raman scattering microscopy. Applied Physics Letters, 2017, 111, 063704.	1.5	7
121	Large eddy simulation of a supersonic lifted hydrogen flame with sparse-Lagrangian multiple mapping conditioning approach. Combustion and Flame, 2022, 238, 111756.	2.8	5
122	<title>Evaluation of variations of biomolecular constituents in human skin in vivo by near-infrared
Raman spectroscopy</title> . , 2001, , .		4
123	Effect of hormonal variation on in vivo high wavenumber Raman spectra improves cervical precancer detection. , 2012, , .		4
124	Phase-controlled polarization coherent anti-Stokes Raman scattering microscopy for high-sensitivity and high-contrast molecular imaging. Journal of the Optical Society of America B: Optical Physics, 2008, 25, 1907.	0.9	3
125	Rapid near-infrared fluorescence excitation–emission matrix spectroscopy for multifluorophore characterization using an acousto-optic tunable filter technique. Journal of Biomedical Optics, 2010, 15, 027010.	1.4	3
126	In vivo Raman spectroscopy integrated with multimodal endoscopic imaging for early diagnosis of gastric dysplasia. , 2010, , .		3

#	Article	IF	CITATIONS
127	Real-time depth-resolved Raman endoscopy for <i>in vivo</i> diagnosis of dysplasia in Barrett's esophagus. Proceedings of SPIE, 2013, , .	0.8	3
128	Simultaneous fingerprint and high-wavenumber fiber-optic Raman endoscopy for <i>in vivo</i> diagnosis of laryngeal cancer. Proceedings of SPIE, 2016, , .	0.8	3
129	Combining raman spectroscopy with background near-infrared autolluorescence to improve the non-invasive detection of malignant tumors. , 0, , .		2
130	Saliva analysis using surface-enhanced Raman spectroscopy technique. , 2007, , .		2
131	Image-guided near-infrared Raman spectroscopy for in vivo detection of gastric dysplasia. Proceedings of SPIE, 2009, , .	0.8	2
132	An integrated coherent anti-Stokes Raman scattering and multiphoton imaging technique for liver disease diagnosis. , 2012, , .		2
133	Integrated fingerprint and high wavenumber confocal Raman spectroscopy for in vivo diagnosis of cervical precancer. Proceedings of SPIE, 2013, , .	0.8	2
134	Integrated coherent Raman scattering and multiphoton microscopy for label-free imaging of the dentin in the tooth. , 2014, , .		2
135	Simultaneous quadruple modal nonlinear optical imaging for gastric diseases diagnosis and characterization. Proceedings of SPIE, 2015, , .	0.8	2
136	Near-infrared Raman spectroscopy for colonic cancer diagnosis. , 2005, , .		1
137	Quantitative analysis of skin chemicals using rapid near-infrared Raman spectroscopy. , 2008, , .		1
138	Radially polarized tip-enhanced near-field coherent anti-Stokes Raman scattering microscopy for bioimaging. , 2012, , .		1
139	Moving Raman spectroscopy into real-time, online diagnosis and detection of precancer and cancerin vivoin the upper GI during clinical endoscopic examination. , 2013, , .		1
140	Quantitative fiber-optic Raman spectroscopy for tissue Raman measurements. , 2014, , .		1
141	36 Fiberoptic Confocal Raman Endoscopy for Enhancing Real-Time In Vivo Diagnosis of Gastric Precancer. Gastroenterology, 2014, 146, S-10.	0.6	1
142	Simultaneous fingerprint and high-wavenumber Raman endoscopy for in vivo diagnosis of colorectal precancer. , 2015, , .		1
143	High-resolution stimulated Raman scattering microscopy by focal-field modulation. Proceedings of SPIE, 2016, , .	0.8	1
144	Hyperspectral stimulated Raman scattering and multiphoton imaging for digital pathology of colonic disease. , 2016, , .		1

#	Article	IF	CITATIONS
145	Near-infrared autofluorescence polarization imaging for colonic cancer detection. , 2009, , .		1
146	<title>Autofluorescence diagnostic algorithm for detecting malignant colonic tissues</title> .,2001, ,.		0
147	Near-infrared Raman spectroscopy detects lung cancer. , 2005, 5630, 340.		Ο
148	Classification of Raman Spectra of Colonic Tissues using Pattern Recognition Technique. , 2006, , ME62.		0
149	Near-infrared Raman spectroscopy for optical diagnosis of gastric precancer. Proceedings of SPIE, 2007, 6826, 431.	0.8	Ο
150	Near-infrared Fluorescence Imaging for Colonic Cancer Diagnosis. , 2007, , .		0
151	A specially modified surface-enhanced Raman spectroscopy (SERS) substrate for biomedical applications. Proceedings of SPIE, 2008, , .	0.8	Ο
152	Raman spectroscopy for optical diagnosis of laryngeal cancer. Proceedings of SPIE, 2008, , .	0.8	0
153	Autofluorescence spectroscopic imaging for laryngeal cancer detection. Proceedings of SPIE, 2008, , .	0.8	Ο
154	Elliptically Polarized Coherent anti-Stokes Raman Scattering Microscopy for High Contrast Vibrational Imaging. , 2009, , .		0
155	Coherent anti-stokes Raman scattering (RP-CARS) microscopy for sensing molecular orientations. Proceedings of SPIE, 2009, , .	0.8	Ο
156	Annular aperture detection scheme in radially polarized coherent anti-Stokes Raman scattering (RP-CARS) microscopy for contrast improvement. Proceedings of SPIE, 2010, , .	0.8	0
157	Multimodal endoscopic imaging and Raman spectroscopy for improving in vivo diagnosis of gastric malignancies during clinical gastroscopy. Proceedings of SPIE, 2010, , .	0.8	Ο
158	Assessment of fibrotic liver disease with multimodal nonlinear optical microscopy. , 2010, , .		0
159	Image-Guided Raman Spectroscopy For In Vivo Diagnosis of Gastric Precancer At Gastroscopy. , 2010, , .		Ο
160	Multimodal nonlinear optical imaging of obesity-induced liver steatosis and fibrosis. , 2011, , .		0
161	High contrast coherent anti-Stokes Raman scattering microscopy using tightly focused cylindrical vector beams. , 2011, , .		0
162	Univariate and multivariate methods for chemical mapping of cervical cancer cells. , 2012, , .		0

#	Article	IF	CITATIONS
163	Detection of malignant lesions in vivo in the upper gastrointestinal tract using image-guided Raman endoscopy. , 2012, , .		0
164	Polarization-coded coherent anti-Stokes Raman scattering microscopy for nonresonant background suppression. Proceedings of SPIE, 2013, , .	0.8	0
165	Simultaneous Fingerprint and High-Wavenumber Confocal Raman Spectroscopy Enables Real-time In Vivo Diagnosis of Colonic Cancer at Endoscopy. , 2014, , .		0
166	Simultaneous stimulated Raman scattering and higher harmonic generation imaging for liver disease diagnosis without labeling. , 2014, , .		0
167	Study of acetowhitening mechanisms in live mammalian cells with label-free subcellular-level multimodal nonlinear optical microscopy. Proceedings of SPIE, 2015, , .	0.8	0
168	Compact Raman needle probe with fine needle aspiration biopsy for solid tissues. Proceedings of SPIE, 2015, , .	0.8	0
169	A novel broadband Raman endoscopy for <i>in vivo</i> diagnosis of intestinal metaplasia in the stomach. Proceedings of SPIE, 2015, , .	0.8	0
170	Glucose sensing through Fano resonances in mesoscale silica core-gold shell particles arrays. Proceedings of SPIE, 2016, , .	0.8	0
171	Near-infrared Mueller matrix imaging for colonic cancer detection. , 2016, , .		0
172	Diagnosis potential of near infrared Mueller Matrix imaging for colonic adenocarcinoma. Proceedings of SPIE, 2016, , .	0.8	0
173	Endoscope-based beveled and volume fiber-optic Raman probes for in vivo diagnosis of gastric dysplasia: a comparative study. , 2016, , .		Ο
174	Dental caries imaging using hyperspectral stimulated Raman scattering microscopy. Proceedings of SPIE, 2016, , .	0.8	0
175	Guest Editorial: Special Topic on Coherent Raman Spectroscopy and Imaging. APL Photonics, 2018, 3, 090401.	3.0	Ο
176	Coherent Anti-Stokes Raman Scattering Microscopy for Sensing Molecular Orientations. , 2009, , .		0
177	Polarization-Resolved Hyperspectral Stimulated Raman Microscopy for Tooth Imaging. , 2016, , .		0
178	Coherent Raman scattering microscopy for superresolution vibrational imaging: Principles, techniques, and implementations. , 2022, , 147-163.		0
179	Fourier-Domain Stimulated Raman Scattering Tomography For Label-Free Deep Tissue Chemical Imaging. , 2022, , .		0